2011 American Control Conference
on O'Farrell Street, San Francisco, CA, USA
June 29 - July 01, 2011

Combined State-Parameter Estimation for Shallow Water Equations

Mohammad Rafiee Andrew Tinka Jerome Thai Alexandre M. Bayen

Abstract— **In this article, a method for assimilating data into the shallow water equations when some of the model parameters are unknown is presented. The one dimensional Saint-Venant equations are used as a model of water flow in open channels. Using these equations, a nonlinear state-space model is obtained. Lagrangian measurements of the flow velocity field are used as observations or measurements. These measurements may be obtained from a group of drifters equipped with GPS receivers and communication capabilities which move with the flow and report their position at every time step. Using the derived state-space model, the *extended Kalman filter* is used to estimate the state and the unknown model parameters given the latest measurements. The performance of the method is evaluated using data collected from an experiment performed at the USDA-ARS Hydraulic Engineering Research Unit (HERU) in Stillwater, Oklahoma in November 2009.**

I. INTRODUCTION

Data assimilation is the process of integrating observations or measurements into a mathematical model of a physical system, in order to estimate some quantities of interest. Recently, data assimilation has provided rapid advances in geosciences such as meteorology, occeanography and hydrology [1], [3], [5], [19]. Different methods for assimilating data include variational data assimilation [6], filtering-based methods [15], [20], optimal statistical interpolation [22], or the Newtonian relaxation [18], [24].

Open channel flow is an example of the so-called *distributed parameter systems*. A physical system which is modelled by a set of *partial differential equations* (PDE) is called a distributed parameter system. For modelling the water flow in rivers and open channels, the Saint-Venant equations, which are a set of first-order hyperbolic nonlinear PDEs, are commonly used [13], [2]. Solving the PDEs requires an accurate knowledge of the boundary conditions, which are usually obtained from measurements of sensors installed at appropriate locations. However, noise and inaccuracies in the measurements of the boundary conditions, as well as modelling assumptions (simplifications made to construct the mathematical model), can lead to mismatch between the model prediction of the system state and the actual state of the system. When additional observations (measurements) of the system state are available, it is desirable to incorporate these measurements into the model to reduce the mismatch between the model prediction and the actual system and improve the model predictions throughout the whole domain of interest.

In this article, we present a method to integrate Lagrangian measurements of the flow into the one dimensional Saint-Venant equations using the *extended Kalman filter* (EKF). *Lagrangian measurements* are measurements of the flow properties at a point moving with the flow along the streamline whereas *Eulerian measurements* are measurements of the flow properties at a fixed location. Lagrangian sensors which move with the flow and report their location and possibly other local quantities of interest (temperature, salinity, etc.) are commonly used in oceanography [7], [16], [26] (usually referred to as *drifters*) and in river hydraulics [4]. Lower production and maintenance cost, as well as flexibility in deployment, are the main advantages of the drifters over the traditional static sensors. These drifters are equipped with GPS receivers and report their position, velocity and other measurements at every time step. The goal is to estimate the state of the system, which consists of the flow and stage throughout the whole domain of interest, i.e. at all discretized cells, using the local velocity measurements of the flow obtained from a number of drifters.

In [25], using linearized one dimensional Saint-Venant equations as the flow model, the Kalman filter is used to estimate the state using the drifter position data. It is shown that the Kalman filter based on the linear model provides accurate estimates when the deviation from the steady state around which the system is linearized is moderate. However, the error significantly increases with time as the deviation of the state of the system from the steady state increases. In the present article, we use nonlinear one dimensional Saint-Venant equations as the model of the flow. Furthermore, it is assumed that some of the model parameters are unknown. In practice, it is sometimes not possible to obtain an accurate approximation of the parameters of the model because of lack of proper equipment, time constraints, costs, etc. As a matter of fact, one of the motivations of using drifters to obtain measurements as opposed to traditional static sensors is their applicability in new areas where no infrastructure is available. For instance, in case of an emergency (e.g. a levee break, gate malfunction), measurements of the flow can be obtained by releasing a group of drifters in the region of interest and use these measurements to model the flow in real time. For such applications, there will not be enough time to design an experiment to identify the model parameters, or even if all the parameters have been identified before, in

M. Rafiee is a Ph.D. candidate in the Department of Mechanical Engineering, University of California, Berkeley, CA 94720 (email: rafiee@berkeley.edu). Corresponding author.

A. Tinka is a Ph.D. candidate in the Department of Electrical Engineering, University of California, Berkeley, CA 94720 (email: tinka@berkeley.edu).

J. Thai is a M.Sc. student in the Department of Industrial Engineering and Operations Research, Columbia University, New York, NY 10027 (email: jht2115@columbia.edu).

A. Bayen is an Associate Professor in Systems Engineering, Department of Civil and Environmental Engineering, University of California, Berkeley, CA 94720 (email: bayen@berkeley.edu).

case of an emergency, the flow conditions (e.g. the channel geometry) may change significantly such that the former values of parameters are no longer accurate enough. One possible approach is to assume a rough approximation of the parameter and perform the data assimilation method. However, depending on the sensitivity of the model to the unknown parameters, the error introduced by these approximations may be large. In the present article, we propose a method to estimate the unknown model parameters along with the state in real time by augmenting the unknown parameters to the state vector and applying the extended Kalman filter to perform state estimation on the augmented state-space model. It is clear considering parameters as unknown as opposed to having fixed values adds to the degrees of freedom of the model and hence may improve the estimation results.

We evaluate the performance of the method using data collected from an experiment performed at the USDA-ARS Hydraulic Engineering Research Unit (HERU) in Stillwater, Oklahoma in November 2009. Since the bottom elevation of the channel is not available, the bed slope of the channel is assumed as an unknown parameter. Compared to the case of performing state estimation assuming a zero bed slope, it is shown that considering the bed slope as an unknown parameter and using the measurements to estimate it improves the model prediction.

The rest of this article is organized as follows. In section II, the Saint-Venant model is presented and the equations are discretized using the Lax diffusive scheme. In section III, a state-space model is constructed and the method to perform combined parameter-state estimation using the extended Kalman filter is described. In section IV, we describe the drifter hardware, software and communication, the experiment setup and specifications and the numerical results. Finally, in section V, we conclude the article.

II. Mathematical Model

A. The Saint-Venant Model

The Saint-Venant model is among the most common models used for modeling the flow in open channels and irrigation systems [13], [2]. In the one dimensional case, Saint-Venant equations are two coupled first-order hyperbolic partial differential equations (PDE) derived from conservation of mass and momentum. For prismatic channels with no lateral inflow, these equations can be written as [27]

$$T\frac{\partial H}{\partial t}+\frac{\partial Q}{\partial x}=0 \tag{1}$$

$$\frac{\partial Q}{\partial t}+\frac{\partial}{\partial x}\left(\frac{Q^2}{A}\right)+\frac{\partial}{\partial x}(gh_cA)=gA(S_0-S_f) \tag{2}$$

for $(x,t)\in(0,L)\times\Re^+$, where L is the river reach (m), $Q(x,t)$ is the discharge or flow (m^3/s) across cross section $A(x,t)=T(x)H(x,t)$, $H(x,t)$ is the stage or water-depth (m), $T(x)$ is the free surface width (m), $D=A/T$ is the hydraulic depth m, $S_f(x,t)$ is the friction slope (m/m), S_b is the bed slope (m/m), g is the gravitational acceleration (m/s^2). The friction slope is empirically modeled by the Manning-Strickler's formula [21]:

$$S_f=\frac{m^2Q^2P^{4/3}}{A^{10/3}} \tag{3}$$

with $Q(x,t)=V(x,t)A(x,t)$ the discharge across cross-section $A(x,t)$, P the wetted perimeter, and m the Manning's roughness coefficient ($sm^{-1/3}$).

The boundary conditions are usually taken to be the upstream flow $Q(0,t)$ and the downstream stage $H(L,t)$.

Remark 1: Throughout this article, we assume the flow to be *sub-critical*, i.e. the *Froude number* defined as $F=V/C$ with $C=\sqrt{gD}$ being the *wave celerity* is less than 1.

Remark 2: The dependence on the spatial variable x is occasionally omitted for the sake of readability.

B. Discretization: Lax Diffusive Scheme

We use the Lax diffusive scheme [12], [27] which is a first-order explicit scheme to discretize the equations. Using f to represent the dependent variables, v and h, the derivatives become

$$\frac{\partial f}{\partial t}=\frac{f_i^{k+1}-\frac{1}{2}(f_{i+1}^k+f_{i-1}^k)}{\Delta t} \tag{4}$$

$$\frac{\partial f}{\partial x}=\frac{(f_{i+1}^k-f_{i-1}^k)}{2\Delta x} \tag{5}$$

using the traditional finite difference discretization notation, with subscript i for space and supperscript k for time.

Applying this scheme to equations (1) and (2), we obtain the set of following finite difference equations,

$$A_i^{k+1}=\frac{1}{2}(A_{i-1}^k+A_{i+1}^k)-\frac{\triangle t}{2\triangle x}(Q_{i+1}^k-Q_{i-1}^k) \tag{6}$$

$$Q_i^{k+1}=\frac{1}{2}(Q_{i-1}^k+Q_{i+1}^k) - \frac{\triangle t}{2\triangle x}\left[\left(\frac{Q^2}{A}+gAh_c\right)_{i+1}^k-\left(\frac{Q^2}{A}+gAh_c\right)_{i-1}^k\right] \tag{7}$$

$$+\triangle t\left(\frac{\phi_{i+1}^k+\phi_{i-1}^k}{2}\right) \tag{8}$$

where

$$\phi=gA(S_b-S_f) \tag{9}$$

This scheme is stable provided that the *Courant-Friedrich-Lewy* (CFL) condition holds, i.e.

$$\frac{\Delta t}{\Delta x}|V+C|\leq 1 \tag{10}$$

The equations above may only be used for interior grid points. At the boundaries, these equations cannot be applied since there is no grid point outside the domain. Therefore, another method needs to be used to compute the unknown variables at the boundaries. Here, we use the *method of specified time intervals* to compute these variables [12]. In this method, after computing the characteristics, the boundary

grid point is projected backward to the previous time step along its corresponding characteristic curve. After computing the variables at the projected point, which is usually done by using linear interpolation, the characteristic equations are used to compute the unknown variable at the boundary grid point at the next time step.

III. Combined State-parameter Estimation

A. State-Space Model

The discretized equations obtained in section II-B can be used to obtain a state-space model

$$x_{k+1} = f(x_k, u_k) \tag{11}$$

where x_k is the state vector at time k

$$x_k = (Q_2^k, \cdots, Q_N^k, H_1^k, \cdots, H_{N-1}^k)^T \tag{12}$$

and the input u_k contains the boundary conditions, i.e. the upstream flow and downstream stage,

$$u_k = (Q_1^k, H_N^k)^T \tag{13}$$

Q_i^k and H_i^k are the flow and stage at cell i at time $k\Delta t$, respectively, and N is the number of cells used for the discretization of the channel.

Assuming that all model parameters are known, when measurements of the flow other than the boundary conditions are available, these measurements can be incorporated into the state-space model using one of the standard nonlinear filters, e.g. the extended Kalman filter. However, in practice, it is sometimes impossible or expensive to obtain accurate values for one or more of these parameters. For instance, it is usually a difficult task to obtain an accurate value for the bed slope of a channel. As it will be shown in section IV-D, the results of the model are very sensitive to the value of the bed slope. In such cases, proper experiments can be designed to obtain measurements of the system and these measurements may be used later to *identify* the unknown parameters. Nevertheless, it is sometimes not possible to carry out this kind of experiments beforehand due to time constraints, lack of proper equipment, high costs, etc.

In order to obtain estimates of the unknown parameters in real time, we augment a vector of unknown parameters v_k to the state vector and consider $v_{k+1} = v_k$ as the time evolution of the parameters. A nonlinear filter can then be applied to the augmented state-space model to simultaneously estimate the parameters and the actual state of the system.

B. Measurement Model

The information of the position of the drifters equipped with GPS can be used to obtain Lagrangian measurements of the flow velocity. Each drifter reports its current position at every time step which is used to calculate the speed of the drifter at every time step. In order to derive the relation between the drifter velocity and the flow at the corresponding cross-section, we assume a quartic velocity profile on the surface and a logarithmic profile along the depth [10]. For a given particle moving at a distance y from the center line and z from the surface, the particle's velocity $v_p(y, z)$ is related to the flow Q with the following equations:

$$v_p(y, z) = F_T(y) F_V(z) \frac{Q}{A} \tag{14}$$

with

$$F_T(y) = A_q + B_q \left(\frac{2y}{w}\right)^2 + C_q \left(\frac{2y}{w}\right)^4 \tag{15}$$

$$A_q + B_q + C_q = 0 \tag{16}$$

$$A_q + \frac{B_q}{3} + \frac{C_q}{5} = 1 \tag{17}$$

$$F_V(z) = 1 + \left(\frac{0.1}{\kappa}\right)\left(1 + log\left(\frac{z}{d}\right)\right) \tag{18}$$

where w is the channel width, d is the water depth, and A_q, B_q and C_q are constants and $\kappa = 0.4$. A_q is commonly calculated experimentally and equations (16) and (17) are used to compute B_q and C_q.

Denoting the collection of velocity measurements obtained from the drifters at time step k by y_k, the measurement model can be written as

$$y_k = g(x_k, k) \tag{19}$$

Note that the observation operator g is time-varying since the drifters are moving with the flow. Therefore, the cells at which the flow velocity is measured are changing over time.

C. Stochastic State-space Model

The effect of modelling uncertainties, as well as inaccuracies in measurements of the inputs, are commonly considered as an additive noise term in the state equations (11) to obtain a stochastic equation

$$x_{k+1} = f(x_k, u_k, w_k) \tag{20}$$

The noise w_k is usually assumed to be zero-mean white Gaussian and

$$E[w_k w_l^T] = Q_k \delta_{kl} \tag{21}$$

$x_0 \in \mathbb{R}^m$ is the initial state which is also assumed to be Gaussian and

$$x_0 = \mathcal{N}(\bar{x}_0, P_0) \tag{22}$$

where $\bar{x}_0$ and P_0 are the initial guesses for state and error covariance.

Similarly, the errors and uncertainties in the measurements can be taken into account by adding a noise term to the measurement model (23) to obtain

$$y_k = g(x_k, e_k, k) \tag{23}$$

where e_k is the measurement noise of the sensors which is assumed to be zero-mean white Gaussian and

$$E[e_k e_l^T] = R_k \delta_{kl} \tag{24}$$

We also assume that the process and measurement noises and the initial conditions are all independent.

D. Extended Kalman Filter

In the *Extended Kalman Filter* (EKF), the states of the system are approximated by a Gaussian random variable and are propagated through a linearized approximation of the state equations. The *prior* mean of the state is fed into the state equations to yield the prediction of the state. The *posterior* covariance matrices are calculated for a linear model which is obtained from linearizing the state equations around the current estimate [9].

With the stochastic state-space model given in the previous section and the following notations

$$\hat{x}_{k|k-1} = \mathbb{E}[x_k|y_0, y_1, \cdots, y_{k-1}] \tag{25}$$

$$\hat{x}_{k|k} = \mathbb{E}[x_k|y_0, y_1, \cdots, y_k] \tag{26}$$

$$P_{k|k-1} = \mathbb{E}[(x_k - \hat{x}_{k|k-1})(x_k - \hat{x}_{k|k-1})^T|y_0, y_1, \cdots, y_{k-1}] \tag{27}$$

$$P_{k|k} = \mathbb{E}[(x_k - \hat{x}_{k|k})(x_k - \hat{x}_{k|k})^T|y_0, y_1, \cdots, y_k] \tag{28}$$

the iterations of the EKF can be summarized as follows

Time update:

$$\hat{x}_{k|k-1} = f(\hat{x}_{k-1|k-1}, u_{k-1}, 0) \tag{29}$$

$$P_{k|k-1} = \Phi_{k-1} P_{k-1|k-1} \Phi_{k-1}^T + B_{k-1} Q_{k-1} B_{k-1}^T \tag{30}$$

Measurement update:

$$K_k = P_{k|k-1} G_k^T (G_k P_{k|k-1} G_k^T + D_k R_k D_k^T)^{-1} \tag{31}$$

$$\hat{y}_k = G_k \hat{x}_{k|k-1} \tag{32}$$

$$\hat{x}_{k|k} = \hat{x}_{k|k-1} + K_k(y_k - \hat{y}_k) \tag{33}$$

$$P_{k|k} = (I - K_k G_k) P_{k|k-1} \tag{34}$$

where

$$\Phi_{k-1} = \left.\frac{\partial f}{\partial x}\right|_{\hat{x}_{k|k-1}, u_{k-1}}, B_{k-1} = \left.\frac{\partial f}{\partial w}\right|_{\hat{x}_{k|k-1}, u_{k-1}} \tag{35}$$

IV. Implementation

A. Sensor Hardware

The Floating Sensor Network project at UC Berkeley (http://float.berkeley.edu) designs and builds drifters for riverine and estuarine environments. Six second-generation drifters were used in this experiment.

Fig. 1: Overview of the drifter hull. Left: closed. Right: open.

The hull is manufactured at UC Berkeley using low-cost, small-run manufacturing techniques. The drifter has a vertical cylinder configuration in order to present a uniform profile to surface currents while also supporting the antennas a small distance above the waterline. The hull consists of four major components, shown in Figure 1: a hand-cast fiberglass lower hull (A), machined aluminum parts for the watertight seal (B), a commercially available fiberglass pipe for the upper hull (C), and a vacuum-formed polycarbonate top cap (D). The lower hull is flooded so that water quality sensors mounted in the bulkhead may contact the water but also be mechanically protected. In order to keep the center of mass below the center of buoyancy (a necessary condition for stability), 800 g of ballast must be located at the bulkhead between the upper and lower hull. The battery that powers the electronics is part of this ballast. Our standard configuration is to use a 200 g battery and a 600 g lead weight. The battery and water quality sensor are labelled (E) in Figure 1.

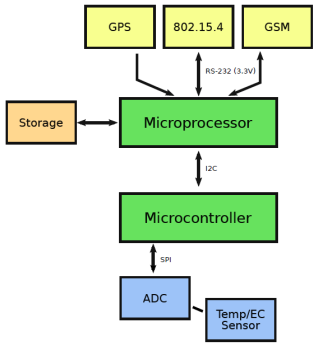

Fig. 2: Module-level block diagram of drifter electronics.

The electronics are mounted near the top of the cylinder. See Figure 2 for a block diagram of the major modules.

The GPS receiver, GSM module, and embedded computer are on the main electronics PCB, labelled (G) in Figure 1. A subordinate microcontroller for real-time tasks such as sensor management is located on a lower board (F). Antennas for the GPS and GSM modules, and a short-range 2.4 GHz radio, are located at the top of the hull (H).

The GPS receiver is the Magellan AC-12 OEM module. In autonomous mode (not using differential correction, SBAS, or post-processing), its Circular Error Probability (CEP) range is 1.5 m [28].

Long-range communication with the server is performed using the Motorola G24 GSM module. In areas with GSM coverage, the General Packet Radio Service (GPRS) service can be used to open TCP or UDP packets to servers on the Internet. Data rates depend on the cellular tower configuration, but are at least 9.6 kbit/s upload and download [23].

Short-range communication between drifters, and between drifters and field personnel, is performed with the Digi XBee-PRO ZB module. Using the IEEE 802.15.4-2006 protocol [17], these devices can form ad-hoc mesh networks. The "PRO" module can transmit with 50 mW (17 dBm) of power [14]; we have observed connectivity at distances of up to 1 km in river environments when using these modules.

The embedded computer is a Gumstix Verdex Pro XM4, a $20\,\mathrm{mm} \times 80\,\mathrm{mm}$ single-board computer with a Marvell PXA270 400 MHz processor and 64 MB of RAM. The PXA270 is an applications processor designed around the ARMv5 architecture. One relevant characteristic for designers of embedded sensor systems is that the PXA270 does not have hardware floating point capability, which may make it difficult to efficiently implement intensive signal processing or other computations. The Verdex is developed to run an OpenEmbedded Linux distribution.

B. Software and Communication

Because of the small experimental domain (and the low probability of losing a drifter), the GSM modules were not activated in this experiment. Instead, GPS position and velocity readings were stored on a 1 GB MicroSD card installed on the Verdex and simultaneously transmitted over the XBee radio to a nearby laptop, which uploaded them to the home server using a database synchronization protocol over a single GSM link. See Figure 3.

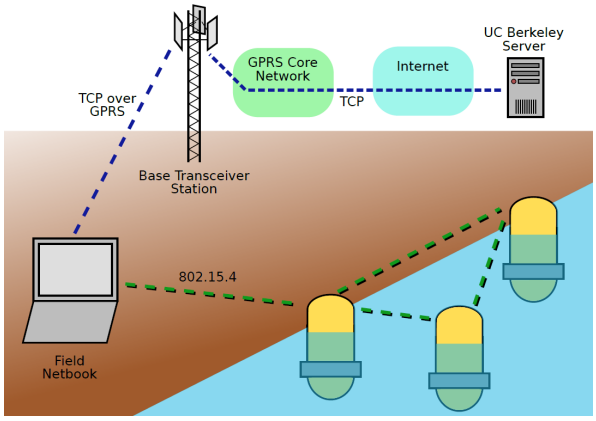

Fig. 3: Communication architecture.

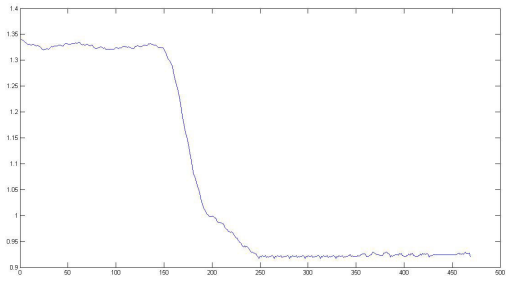

Fig. 4: The downstream stage (m).

C. Mission Description

In November 2009, an experiment was performed at the USDA-ARS Hydraulic Engineering Research Unit (HERU) in Stillwater, Oklahoma. The HERU facility, located adjacent to Lake Carl Blackwell, has a gravity-fed supply canal which can have a controlled rate of up to 4.25 m^3/s (150 ft^3/s). The supply canal feeds a number of experimental units which are normally used for investigations into levee reliability, reservoir safety, and spillway design [11]. For our experiment, we deployed drifters into the supply canal itself. The upstream boundary condition was the supply canal flow control, set to 1.42 m^3/s (50 ft^3/s); the downstream boundary condition was a gate that could be raised or lowered to restrict the flow out of the experimental region. In this experiment, the downstream gate was opened as soon as the final drifter was released. The water stage was captured at the downstream boundary with a video camera. Figure 4 shows the stage at the downstream end of the channel. As can be seen in this figure, the downstream stage is initially 1.33 m and it starts to decrease as the downstream gate is opened until it becomes 0.92m.

Drifters were released at approximately 30 s intervals near the upstream boundary, at point A in Figure 5. After travelling through the canal for approximately 400 s, they were individually retrieved at point B. Point C marks the location of the downstream control gate.

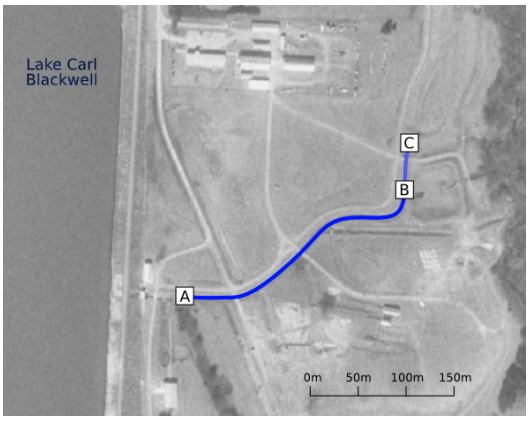

Fig. 5: HERU facility, with experimental channel annotated. Image courtesy of USGS.

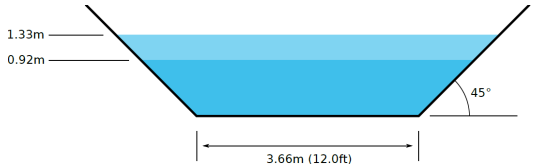

Fig. 6: Channel profile, including minimum and maximum water height.

Fig. 7: Two drifters in the HERU facility supply canal.

Figure 6 shows the cross section of the prismatic channel over most of its extent.

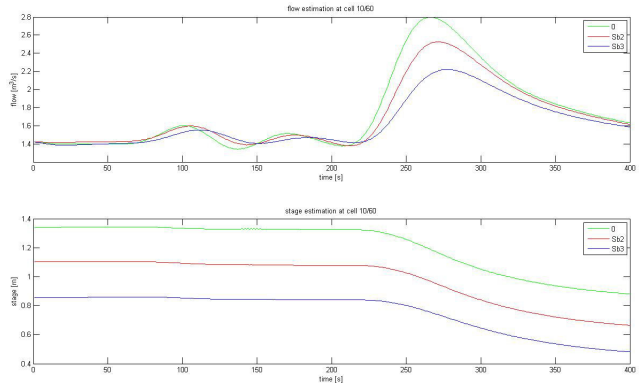

Fig. 8: The flow (top) and stage (bottom) at the 10^{th} cell for $S_b = 0$ (green), $S_b = 0.001$ (red), $S_b = 0.002$ (blue).

D. Numerical Results

The discretization is done by dividing the channel to 60 cells and the temporal step size is chosen as 1 s. Since we do not have any data about the bottom elevation of the channel, we cannot calculate the bed slope of the channel. In order to determine the sensitivity of the model with the given boundary conditions to the value of the bed slope, we run the forward simulation with three different values of bed slope. In each case, the initial condition is chosen to be the backwater curve (steady state) which is computed using the following equations:

$$\frac{\partial Q}{\partial x} = 0 \tag{36}$$

$$\frac{\partial H}{\partial x} = \frac{gA(S_0 - S_f)}{-Q^2 \frac{T_b + 2H}{H^2(T_b+H)^2} + g(T_b H + H^2)} \tag{37}$$

where T_b is the bottom width.

Figure 8 shows the flow and stage at the 10^{th} cell for the three values of bed slope. It is not surprising to see that the results of forward simulation varies significantly with different values of the bed slope.

To implement the data assimilation method, we use the measurements obtained from 5 drifters. We then estimate the velocity of the 6^{th} drifter using the estimated flow which we compare with its actual value obtained from the 6^{th} drifter. We implement the extended Kalman filter with and without estimating the bed slope. Figure 9 shows the flow and stage at a few different cells predicted by the forward simulation (i.e. state-space model) assuming the bed slope is zero, estimated flow and stage by performing the data assimilation method while the bed slope is assumed to be zero, and estimated flow and stage by performing the data assimilation method and estimating the bed slope as an unknown parameter. As can be seen in Figure 4, the downstream stage starts to decrease at around time step 150 due to the gate opening. As can be seen in Figure 9, the flow increases as a result of opening the gate. It can be seen in Figure 9 that the stage reduction caused by opening the gate propagates backward through the channel. However, in case of assuming the bed slope as an unknown parameter, this reduction is stage is more moderate. In particular, at cell 10, no decrease in the stage is seen. This is due to the fact that for a nonzero bed slope, the backwater curve (steady state) is not uniform. Since the initial estimate of the bed slope is taken to be equal to zero, the extended Kalman filter is initialized by a uniform steady state corresponding to a zero bed slope. However, as the estimated bed slope deviates from zero, the steady state of the system deviates from uniform steady state accordingly. While the values of flow and stage estimated by the data assimilation methods seem physically more reasonable, it is not possible to formally evaluate the performance of the method by looking at these figures. In order to obtain a more quantifiable assessment of the method, we calculate the velocity of the 6^{th} drifter using the estimated flow at the corresponding cell. We use the same velocity profiles on the surface and along the depth as described in section III-B to calculate the drifter velocity from the estimated flow. Figure 10 shows the velocity of the 6^{th} drifter predicted by the forward simulation and both data assimilation methods as well as its actual value. As can be seen in this figure, the data assimilation methods significantly improve the estimation results. Also, it can be seen that considering the bed slope as an unknown parameter and using the measurements to estimate it improves the estimation results further.

V. Conclusion

In this article, we presented a method to assimilate measurements obtained from a distributed parameter system into the mathematical model. With the objective of modelling the water flow in an open channel, we used one dimensional Saint-Venant equations as the mathematical model. The Saint-Venant equations, which are a set of PDEs, are used to obtain a state-space model of the flow whose inputs are the boundary conditions. As observations or measurements, we used Lagrangian measurements of the flow velocity field. These measurements are obtained from a group of drifters equipped with GPS receivers and communication capabilities which move with the flow and report their position at every time step. The position data are then used to calculate the drifter velocity. Assuming a quartic velocity profile on the surface and a logarithmic profile along the depth, the drifter velocities are used to compute the flow at the corresponding cross sections. The extended Kalman filter was used to estimate the state of the system given the measurements obtained from the drifters.

We also considered a case where some of the model parameters are unknown. A method was proposed to use the measurements to estimate the unknown parameters along with the state in real time. This is done by artificially augmenting the unknown parameters to the state vector and using the augmented state-space model with the extended Kalman filter.

The numerical results of implementing these methods on data obtained from an experiment done on a 290-meter channel in Stillwater, Oklahoma in November 2009 were presented. Since the bottom elevations were not available to us, it was not possible to compute the value of the bed slope of the channel. We implemented the data assimilation method

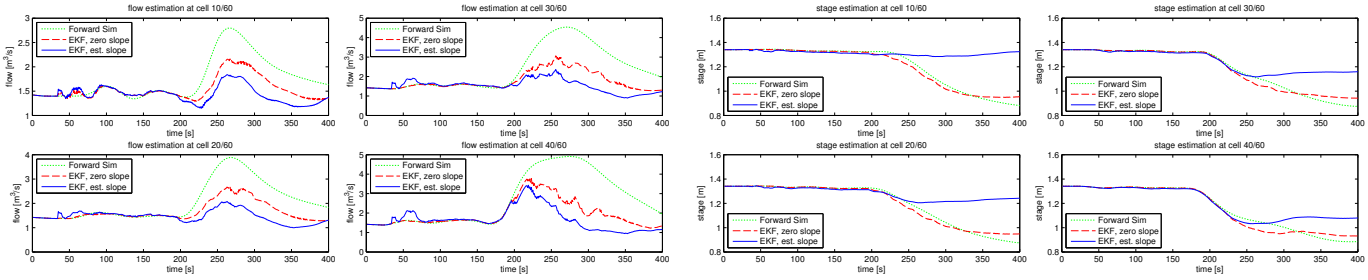

Fig. 9: The flow (m^3/sec) (left) and stage (m) (right) at the 10^{th}, 20^{th}, 30^{th}, 40^{th} cells, forward simulation (green), EKF with zero bed slope (red), EKF with estimating bed slope (blue).

with assuming a zero bed slope and also with considering the bed slope as an unknown parameter. It was shown that using the measurements to estimate the bed slope along with the state improve the results significantly.

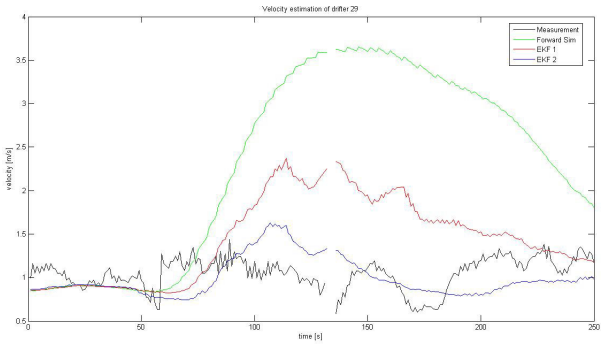

Fig. 10: the velocity of the 6th drifter, forward simulation (green), EKF with zero bed slope (red), EKF with estimating bed slope (blue) and the actual drifter measurements (black).

VI. ACKNOWLEDGMENTS

Xavier Litrico from CEMAGREF is gratefully acknowledged for fruitful discussions during his stay at Berkeley, which shaped the framework used for modeling shallow water, which follow from his work.

REFERENCES

[1] P. Brasseur and J.C.J. Nihoul . Data assimilation: Tools for modelling the ocean in a global change perspective. *In NATO ASI Series, Series I: Global Environmental Change*, 19(239), 1994.

[2] J.A Cunge, F.M. Holly, and A. Verwey. *Practical aspects of computational river hydraulics*. Pitman, 1980.

[3] D.B. Haidvogel and A.R. Robinson . Special issue on data assimilation. *Dyn. Atmos. Oceans*, 13:171–517, 1989.

[4] M. Honnorat, J. Monnier, and F.X.L. Dimet. Lagrangian data assimilation for river hydraulics simulations. In *European Conference on Computational Fluid Dynamics*, Dec 2006.

[5] P. Malanotte-Rizzoli. Modern approaches to data assimilation in ocean modeling. *Elsevier Oceanography Series*, 1996.

[6] I.M. Navon. Practical and theoretical aspects of adjoint parameter estimation and identifiability in meteorology and oceanography. *Dyn. Atmos. Oceans*, (27), 1997.

[7] M. Nodet. Variational assimilation of lagrangian data in oceanography. *Inverse Problems*, 22:245–263, 2006.

[8] O.-P. Tossavainen, J. Percelay, A. Tinka, Q. Wu, and A. Bayen. Ensemble kalman filter based state estimation in 2d shallow water equations using lagrangian sensing and state augmentation. In *Proceedings of the 46th IEEE Conference on Decision and Control*, Dec 2008.

[9] B.D.O. Anderson and J.B. Moore. *Optimal Filtering*. Prentice-Hall, 1979.

[10] Gilbert V. Bogle. Stream velocity profiles and longitudinal dispersion. *Journal of Hydraulic Engineering*, 123(9):816–820, 1997.

[11] Sherry L. Britton, Gregory J. Hanson, and Darrel M. Temple. A historic look at the USDA-ARS hydraulic engineering research unit. In Glenn O. Brown, Jurgen D. Garbrecht, and Will H. Hager, editors, *Henry P.G. Darcy and other pioneers in hydraulics: contributions in celebration of the 200th birthday of Henry Philibert Gaspard Darcy*, pages 263–276. American Society of Civil Engineers, 2003.

[12] M.H. Chaudhry. *Open-Channel Flow*. Springer, 2008.

[13] V. Chow. *Open-channel Hydraulics*. McGraw-Hill Book Company, New York NY, 1988.

[14] Digi International. *XBee/XBee-PRO ZB RF Modules*, 2009.

[15] G. Evensen. *Data Assimilation: The Ensemble Kalman Filter*. Springer-Verlag, 2007.

[16] S. Fan, L.Y. Oey, and P. Hamilton. Assimilation of drifter and satelite data in a model of the northeastern gulf of mexico. *Continental Self Research*, 24:1001–1013, 2004.

[17] IEEE Std. *IEEE Standard for Information technology - Telecommunications and information exchange between systems - Local and metropolitan area networks - Specific requirements. Part 15.4: Wireless Medium Access Control (MAC) and Physical Layer (PHY) Specifications for Low-Rate Wireless Personal Area Networks (WPANs)*, 2006.

[18] Y. Ishikawa, T. Awaji, K. Akitomo, and B. Qiu. Successive correction of the mean sea surface height by the simultaneous assimilation of drifting buoy and altimetric data. *J. Phys. Oceanogr.*, (26):2381–2397, 1996.

[19] E. Kalnay. *Atmospheric Modeling, Data Assimilation and Predictability*. Cambridge University Press, 2003.

[20] L. Kuznetsov, K. Ide, and C.K.R.T. Jones. A method for assimilation of lagrangian data. *Mon. Wea. Rev.*, 131(10):2247–2260, 2003.

[21] X. Litrico and V. Fromion. *Modeling and Control of Hydrosystems*. Springer, 2009.

[22] A. Molcard, L.I. Piterbarg, A. Griffa, T. Ozgokmen, and A. Mariano. Assimilation of drifter observations for the reconstruction of the eulerian circulation field. *J. Geophys. Res.*, 108(C3), 2003.

[23] Motorola. *Motorola G24 Developers' Guide: Module Hardware Description*, 2007.

[24] C. Paniconi, M. Marrocu, M. Putti, and M. Verbunt. Newtonian nudging for a richards equation-based distributed hydrological model. *Adv. Water. Resour.*, 26(2):161–178, 1996.

[25] M. Rafiee, Q. Wu, and A. Bayen. Kalman filter based estimation of flow states in open channels using lagrangian sensing. In *Proceedings of the 48th IEEE Conference on Decision and Control*, Shanghai, China, Dec 2009.

[26] H. Salman, L. Kuznetsov, and C. Jones. A method for assimilating lagrangian data into a shallow-water-equation ocean model. *Monthly Weather Review*, 134:1081–1101, 2006.

[27] T.W. Strum. *Open Channel Hydraulics*. McGraw-Hill, 2001.

[28] Thales Navigation. *A12, B12, & AC12 Reference Manual*, 2005.